Chinese Chemical Letters 34 (2023) 107651

Contents lists available at ScienceDirect

Chinese Chemical Letters

journal homepage: www.elsevier.com/locate/cclet

Bio-assembled smart nanocapsules for targeted delivery of KRAS shRNA and cancer cell bioimage

Maonan Wang[a], Zengchao Guo[a], Jiayu Zeng[a], Liu Liu[a], Yihan Wang[a], Jinpeng Wang[a], Hongbing Lu[b], Haijun Zhang[c], Hui Jiang[a], Xuemei Wang[a,*]

[a] State Key Laboratory of Bioelectronics (Chien-Shiung Wu Lab), School of Biological Science and Medical Engineering, Southeast University, Nanjing 210096, China
[b] Department of Biomedical Engineering/Computer Application, Fourth Military Medical University, Xi'an 710032, China
[c] Department of Oncology, Zhongda Hospital, Medical School of Southeast University, Nanjing 210009, China

ARTICLE INFO

Article history:
Received 26 December 2021
Revised 25 June 2022
Accepted 27 June 2022
Available online 1 July 2022

Keywords:
Smart bio-responsive nanocapsules
Intelligent nanomedicine
shRNA
KRAS
Fluorescent bioimaging
Oxidative stress response

ABSTRACT

The five-year survival rate for pancreatic cancer is less than 5%. However, the current clinical multimodal therapy combined with first-line chemotherapy drugs only increases the patient's median survival from 5.0 months to 7.2 months. Consequently, a new strategy of cancer treatments is urgently needed to overcome this high-fatality disease. Through a series of biometric analyses, we found that KRAS is highly expressed in the tumor of pancreatic cancer patients, and this high expression is closely related to the poor prognosis of patients. It shows that inhibiting the expression of KRAS has great potential in gene therapy for pancreatic cancer. Given those above, we have exploited the possibility of targeted delivery of KRAS shRNA with the intelligent and bio-responsive nanomedicine to detect the special oxidative stress microenvironment of cancer cells and realize efficient cancer theranostics. Our observations demonstrate that by designing the smart self-assembled nanocapsules of melanin with fluorescent nanoclusters we can readily achieve the bio-recognition and bioimaging of cancer cells in biological solution or serum. The self-assembled nanocapsules can make a significant bio-response to the oxidative stress microenvironment of cancer cells and generate fluorescent zinc oxide Nanoclusters *in situ* for targeted cell bioimaging. Moreover, it can also readily facilitate cancer cell suppression through the targeted delivery of KRAS shRNA and low-temperature hyperthermia. This raises the possibility to provide a promising theranostics platform and self-assembled nanomedicine for targeted cancer diagnostics and treatments through special oxidative stress-responsive effects of cancer cells.

The results of the latest Global Cancer Statistics Report in 2018 show that pancreatic cancer has risen to the top 7 cancer types with the highest mortality rate [1]. Pancreatic cancer is an extremely dangerous and highly malignant tumor of the digestive tract [2–4]. KRAS gene mutations are present in more than 80% of pancreatic cancer patients [5,6]. At present, siRNA and shRNA are mainly used to suppress oncogenes *in vitro* [7,8]. Alternatively, shRNA is more widely used due to its long-acting time and not easy to be degraded. In this work, shRNA is introduced into cells through the vector, in which the U6 promoter inside ensures that the shRNA is expressed; this shRNA-loaded vector can be delivered to the progeny cells so that gene silencing can be inherited. Nanomedicine has achieved solid tumor treatment effects in realizing DNA/RNA delivery *in vivo* [9,10]. At present, there is no nano-delivery system that can achieve targeted delivery of shKRAS. Therefore, recognizing the targeted delivery of shKRAS is a breakthrough in the field of nucleic acid delivery and a better treatment method for pancreatic cancer. Based on this, we designed a nanocapsule (NC) that could achieve targeted delivery of shKRAS and improve NCs' tumor-killing effect by introducing melanin nanoparticles (MNPs). Melanin is an amorphous and irregular biopolymer. It is a ubiquitous natural pigment and exists in many organisms, including human skin [11,12]. MNPs with good water solubility have the following advantages including good biocompatibility, as well as strong absorption at 808 nm, which can realize photothermal treatment or photoacoustic imaging. Based on these considerations, we explored the possibility to use melanin to adsorb Zn^{2+} and Fe^{2+}, which may not only efficiently realize the *in-situ* biosynthesis of ZnO Nanoclusters with fluorescence and Fe_3O_4 nanoclusters but also can realize photothermal therapy si-

* Corresponding author.
E-mail address: xuewang@seu.edu.cn (X. Wang).

https://doi.org/10.1016/j.cclet.2022.06.074
1001-8417/

multaneously [13,14]. In general, the fluorescent NCs put forward new ideas for the clinical treatment of pancreatic cancer.

KRAS mutations can cause continuous activation with GTP, activate downstream pathways, and promote cancer cell occurrence and development [15–19]. The data from Cancer Cell Line Encyclopedia also showed that KRAS has the highest mutation frequency in pancreatic cancer (Fig. S1 in Supporting information), which may mean that KRAS mutation is one of the leading causes of pancreatic cancer. At the same time, the analysis of unpaired (Fig. S2a in Supporting information) and paired (Fig. S2b in Supporting information) cancer and adjacent clinical samples have shown that KRAS is highly expressed in pancreatic cancer and this high expression is significantly related to the poor prognosis of patients with pancreatic cancer (Fig. S3a in Supporting information). Therefore, inhibiting or completely silencing the expression of KRAS is very likely to significantly improve the survival time of patients with pancreatic cancer. A result of NGS sequencing of 11,951 tumor tissue (FFPE) samples collected from multiple centers in China from November 2016 to July 2019 showed that the KRAS gene mutations were mainly concentrated in codons 12, 13, and 61 positions. Among them, mutations at the 12th codon position accounted for more than 80%, including G12A, G12C, G12D, G12R, G12S, and G12V[15] (Fig. S3b in Supporting information). Therefore, research on-site 12 may better mimic the mutation of KRAS *in vivo*. Thus, in subsequent experiments, we used PANC-1 ($KRAS^{G12}$) and CAPRN-2 ($KRAS^{G12}$) pancreatic cancer cell lines for analysis and research.

Referring to the methods of the Zhen Cheng group, we synthesized water-soluble MNPs with 2 nm diameters (Fig. S4a in Supporting information) [11,20]. At the same time, the photothermal effect was detected (Fig. S4b in Supporting information). We also found that MNPs could absorb Fe^{2+} and Zn^{2+} at an appropriate concentration of 1 μmol (Fig. S4c in Supporting information), and the encapsulation rate was 61.16%. After electrostatic adsorption, MNPs and shRNA combine to form a complex. Through the natural grasping ability of chitosan to nucleic acids [21,22], under high-speed oscillation, "nano-spheres" can be formed (Figs. S4d and S5a in Supporting information). Here we find that when the *N/P* ratio is 0.02, chitosan has a better ability to grab shRNA and will not cause a large amount of shRNA to leak. It is quite different from the traditional *N/P* ratio (Eq. 1), which may be caused by the introduction of melanin and other metal cations.

$$N/P = (330 \times A \times D\%)/(164 \times B) \quad (1)$$

In this formula, *N* is the amino group in chitosan; *P* is the phosphate in DNA; *A* is the quality of chitosan; *B* is the treatment of DNA; *D%* is the degree of deacetylation of chitosan.

To improve tumor targeting, we cover the surface of the nanosphere with hyaluronic acid (HA). This is the last step in the synthesis of NCs (Fig. 1a). The corresponding ZETA potential is shown in Fig. S5b (Supporting information). TEM image was shown in Fig. S6a (Supporting information). Through EDS (Figs. S6b and c in Supporting information), we can see that the capsule contains Zn and Fe. Fourier transform infrared spectroscopy [23,24] results (Fig. S6d in Supporting information) show that HA is indeed wrapped in the outer layer of chitosan. The superiority of HA is mainly reflected in its good biocompatibility, biodegradability, and special CD44 receptor binding ability [25–27]. Targeting CD44 can also inhibit the development of cancer cells [28].

Through MTT cytotoxicity experiments, we found that the optimal concentration of NCs in cells was 2.1 mg/mL (Fig. S7a in Supporting information), and when cells are cultured at this concentration, they have a better photothermal effect (Fig. S7b in Supporting information). The use of mild PTT (temperature below 45 °C) could achieve the treatment of tumors without side effects [29].

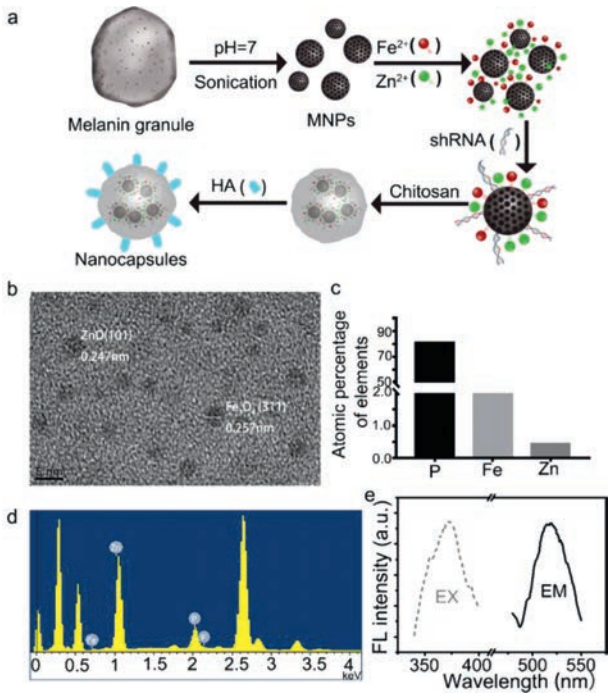

Fig. 1. The synthesis process of nanocapsules. (a) Self-assembled process of NCs; HR-TEM, EDS, EX, and EM of cell extracts after being treated with NCs were shown in (b-e), respectively.

In previous studies, we found that when Zn^{2+} and Fe^{2+} are added to tumor cells, they will be reduced by the reducing substances surrounding the tumor cells, and it is easy to generate fluorescent ZnO nanoclusters and Fe_3O_4 nanoclusters [30–32]. In this case, Fe^{2+} could help the tumor environment to provide more OH^- for ZnO formation. The specific synthesis principle is as follows (Eqs. 2–5):

$$Fe^{2+} + H_2O_2 \rightarrow Fe^{3+} + OH^- + {}^{\bullet}OH \quad (2)$$

$$Fe^{2+} + {}^{\bullet}OH \rightarrow Fe^{3+} + OH^- \quad (3)$$

$$2Fe^{3+} + Fe^{2+} + 8OH^- \rightarrow Fe_3O_4 + 4H_2O \quad (4)$$

$$Zn^{2+} + 2OH^- \rightarrow ZnO + H_2O \quad (5)$$

The *in-situ* synthesis of corresponding nanoclusters of different metal ions at the tumor site brings new hope for targeted therapy and imaging of tumors [9]. Based on this research foundation, after co-cultivating the NCs with tumor cells, we extracted the lysate and found that ZnO and Fe_3O_4 nanoclusters were indeed produced (Figs. 1b-d, Figs. S7c and d in Supporting information). At the same time, we found that it also has good fluorescence characteristics, which is consistent with our research results (Fig. 1e). Immediately afterward, we verified the fluorescence characteristics at the cell level, and the confocal results may verify that the fluorescence is generated by ZnO Nanoclusters synthesized *in situ* by Zn^{2+} in cancer cells (Fig. S8 in Supporting information). In detail, seven experimental groups and one control group were designed to demonstrate the effects of each of the different components in the NCs. When incubated with two cancer cell lines (CAPRN-2, PANC-1) and different NCs, respectively, only the cells with *in situ* synthesized ZnO Nanoclusters were fluorescent, namely HA-ch-shRNA-m-Zn-Fe, HA-ch-shNC-m-Zn-Fe, and HA-ch-shRNA-m-Zn. Meanwhile,

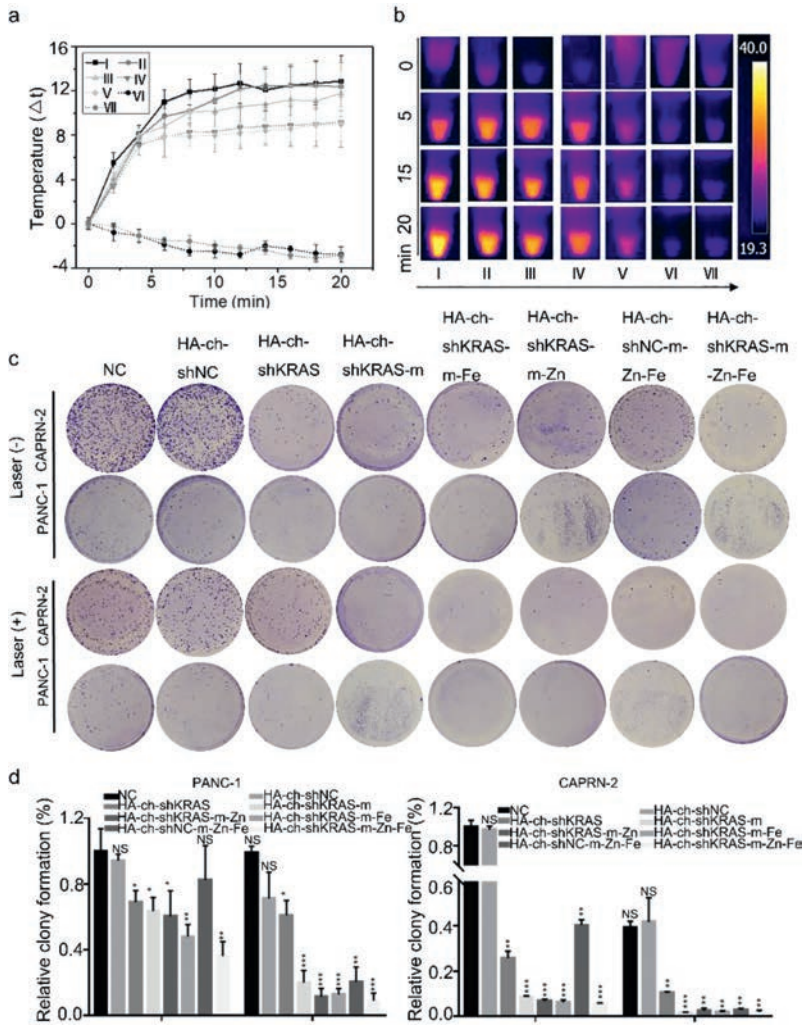

Fig. 2. Low-temperature PTT of nanocapsules. (a) The photothermal effect of cells treated with different reagents and the image result was shown in (b): I. HA-ch-shKRAS-m-Zn-Fe; II. HA-ch-shNC-m-Zn-Fe; III. HA-ch-shKRAS-m-Zn; IV. HA-ch-shKRAS-m-Fe; V. HA-ch-shKRAS-m; VI. HA-ch-shKRAS; VII. HA-ch-shNC. (c) Cloning formation assay of cells treated with different reagents, and the last two lines were also treated with 808 nm laser. The statistical results are reflected in (d). $^{*}P < 0.05$; $^{**}P < 0.01$; $^{***}P < 0.001$; NS, No significant. "HA" stands for hyaluronic acid, and "ch" stands for chitosan.

the fluorescence intensity of HA-ch-shRNA-m-Zn was weaker compared to the other two groups, which was consistent with the previous analysis that the addition of Fe ions promoted the synthesis of more Zn oxide Nanoclusters by Zn ions.

As long as the experimental group contains MNPs, there will be an excellent photothermal effect. A certain amount of NCs in the cells can make the cell temperature rise to about 40 °C (Figs. 2a and b), which is a recognized mild heat therapy temperature that does not cause side effects such as heat shock [33]. The clone formation rate can well reflect the cell viability and proliferation ability [34,35]. Therefore, we used clone formation experiments to detect the deadly effect of NCs on tumor cells (Figs. 2c and d).

The experimental results showed that after laser irradiation, the cells in the experimental group containing melanin died in a large area. After laser irradiation, the clone formation rate is even lower than 0.1%. Without knowing the location of the metastasis, we cannot perform accurate photothermal therapy, and this is where we can use gene therapy to play a role. First, we verified the expression of KRAS at the protein and mRNA levels after the cells were incubated with different NCs (Figs. S9a and b in Supporting information). We found that NCs could deliver shRNA, which may explain the different clone formation rates of the experimental group without laser irradiation in the clone formation experiment. After the expression of the oncogene, KRAS is inhibited, the proliferation ability of tumor cells is significantly weakened, and the clone formation rate is also considerably reduced, which is consistent with the current research results [36,37]. Therefore, through Transwell experiments with/without gel, we tested the invasion and vertical migration capabilities of different NCs (Fig. S9c in Supporting information). The results showed that the delivery of KRAS shRNA could significantly inhibit the invasion and migration ability of tumor cells.

Cancer cells inevitably need to use blood as a bridge in the process of metastasis. The blood of tumor patients is often filled with a certain amount of cancer cells, and there is also a blood microenvironment suitable for the survival and landing of cancer cells. The entry of cancer cells into the blood is the first step for cancer to develop distant metastasis. Therefore, we selected fresh blood from patients with advanced pancreatic cancer to test the fluorescent targeting of the capsules (Fig. S10 in Supporting information), and this result showed that the NCs could function normally in the blood of cancer patients. Patients' blood was sourced from the Zhongda Hospital Southeast University, and

the experiment was approved by the Ethics Committee of Southeast University and the volunteers gave their informed consent. This provides an initial exploration of further applications of NCs in patients.

In summary, we have designed the fluorescent targeted NCs for synergistic cancer cell theranostics via shKRAS delivery and photothermal effects, without introducing exogenous elements. The biocompatibility and *in vivo* metabolic safety of the NCs are more easily understood. Our observations demonstrate that the as-prepared NCs can readily achieve passive transportation in the body, while the HA on the surface could actively bind to the surface antigen CD44 of cancer cells. This active and passive mode of transportation can jointly enhance its drug delivery efficiency *in vivo*. This raises the possibility to provide a new platform for the efficient delivery of shRNA *in situ*, indicating the relevant potential in medical applications. The multi-modal treatment method can kill pancreatic cancer cells by 99.9% *in vitro*. This brings a new promising way for the treatment of pancreatic cancer by inhibiting the expression of the KRAS.

Declaration of competing interest

The authors declare that they have no known competing financial interests or personal relationships that could have appeared to influence the work reported in this paper.

Acknowledgments

This work was supported by the National Natural Science Foundation of China (Nos. 82061148012, 82027806, 91753106), the National Key Research and Development Program of China (No. 2017YFA0205300), the Primary Research & Development Plan of Jiangsu Province (No. BE2019716) as well as the program of China Scholarships Council (No. 202006090323).

Supplementary materials

Supplementary material associated with this article can be found, in the online version, at doi:10.1016/j.cclet.2022.06.074.

References

[1] F. Bray, J. Ferlay, I. Soerjomataram, et al., CA Cancer J. Clin. 68 (2018) 394–424.
[2] S. Sun, Y. Liu, C. He, et al., Cancer Lett. 502 (2021) 9–24.
[3] J.F. Zhang, H.Z. Wang, Pancreas 49 (2020) 1440-1440.
[4] J. Huang, V. Lok, C. Ngai, et al., Trends in Pancreatic Cancer 160 (2021) 744–754.
[5] F. Maire, S. Micard, P. Hammel, et al., Brit. J. Cancer 87 (2002) 551–554.
[6] S. Li, A. Balmain, C.M. Counter, Nat. Rev. Cancer 18 (2018) 767–777.
[7] B. Doiron, W. Hu, L. Norton, R.A. DeFronzo, Diabetologia 55 (2012) 719–728.
[8] T. Kokuryo, S. Hibino, K. Suzuki, et al., Cancer Sci. 107 (2016) 1315–1320.
[9] M. Wang, Y. Chen, W. Cai, et al., Proc. Natl. Acad. Sci. U. S. A. 117 (2020) 308.
[10] Y. Lei, L. Tang, Y. Xie, et al., Nat. Commun. 8 (2017) 15130.
[11] Q. Fan, K. Cheng, X. Hu, et al., J. Am. Chem. Soc. 136 (2014) 15185–15194.
[12] X. Wang, J. Sheng, M. Yang, Chin. Chem. Lett. 30 (2019) 533–540.
[13] F.Rehman Tayyaba, S. Shaikh, et al., J. Mater. Chem. B 8 (2020) 2845–2855.
[14] Y. Wang, H. Feng, H. Zhang, et al., Analyst 145 (2020) 1294–1301.
[15] R.J.C. Slebos, J.A. Hoppin, P.E. Tolbert, et al., Cancer Epidemiol. Biomarkers Prev. 9 (2000) 1223.
[16] H.H. Loong, N. Du, C. Cheng, et al., Transl. Lung Cancer Res. 9 (2020) 1759–1769.
[17] R. Salgia, R. Pharaon, I. Mambetsariev, A. Nam, M. Sattler, Cell Reports Medicine 2 (2021) 100186.
[18] H. Ijichi, A. Chytil, A.E. Gorska, et al., Genes Dev. 20 (2006) 3147–3160.
[19] J. Gout, R.M. Pommier, D.F. Vincent, et al., Pancreatology 13 (2013) 191–195.
[20] J. Lin, M. Wang, H. Hu, et al., Adv. Mater. 28 (2016) 3273–3279.
[21] K. Morikawa, Y. Masubuchi, Y. Shchipunov, A. Zinchenko, ACS Appl. Bio. Mater. 4 (2021) 1823–1832.
[22] T. Tran, N. Amalina, W. Cheow, K. Hadinoto, J. Drug Deliv. Sci. Tec. 59 (2020) 101866.
[23] D. Wang, Y. Xin, Y. Wang, et al., Chem. Eng. J. 409 (2021) 128082.
[24] D. Wang, Y. Xin, X. Li, et al., Chem. Eng. J. 416 (2021) 127625.
[25] Z. Hu, S. Wang, Z. Dai, H. Zhang, X. Zheng, J. Mater. Chem. B 8 (2020) 5351–5360.
[26] H. Cho, H. Yoon, H. Koo, et al., Biomaterials 32 (2011) 7181–7190.
[27] G. Nabil, R. Alzhrani, H. Alsaab, et al., Cancers (Basel) 13 (2021) 898.
[28] R.H. Ateya, A.S. Sultan, Cancer Res. 81 (Suppl. 4) (2021) PS19–PS26.
[29] G. Gao, Y. Jiang, Y. Guo, et al., Adv. Funct. Mater. 30 (2020) 1909391.
[30] T. Du, C. Zhao, F. Rehman, et al., Adv. Funct. Mater. 27 (2016) 1603926.
[31] L. Lai, C. Zhao, M. Su, et al., Biomater. Sci. 4 (2016) 1085–1091.
[32] S. Shaikh, M. Younis, F. Rehman, H. Jiang, X. Wang, Langmuir 36 (2020) 9472–9480.
[33] P. Gao, H. Wang, Y. Cheng, Chin. Chem. Lett. 33 (2022) 575–586.
[34] L. Chibaya, B. Karim, H. Zhang, S. Jones, Proc. Natl. Acad. Sci. U. S. A. 118 (2021) e2003193118.
[35] J.M. Replogle, W. Zhou, A.E. Amaro, et al., Proc. Natl. Acad. Sci. U. S. A. 117 (2020) 30566.
[36] J. Vitos-Faleato, S.M. Real, N. Gutierrez-Prat, et al., Proc. Natl. Acad. Sci. U. S. A. 117 (2020) 2588.
[37] J. Xie, L. Xia, W. Xiang, et al., Proc. Natl. Acad. Sci. U. S. A. 117 (2020) 13012.